Journal of Organometallic Chemistry, 456 (1993) 279–286

JOM 23613

Molecular structure of the compound $[Rh_2(O_2CCH_3)_3\{(C_6H_4)P(BrC_6H_4\text{-}1,2)(C_6H_5)\}\cdot(HO_2CCH_3)_2]$. Kinetic study of the exchange reaction of acetate groups with CD_3CO_2D

P. Lahuerta, J. Latorre, E. Peris and M. Sanaú

Departamento de Química Inorgánica, Universitat de Valencia, Dr. Moliner 50, E-46100 Burjassot-Valencia (Spain)

S. García-Granda

Departamento de Química Física y Analítica, Universidad de Oviedo, Julian Clavería s/n, E-33006 Oviedo (Spain)

(Received December 16, 1992)

Abstract

The compound $[Rh_2(O_2CCH_3)_3\{(C_6H_4)P(BrC_6H_4\text{-}1,2)(C_6H_5)\}\cdot(HO_2CCH_3)_2]$ has been isolated in high yield from the thermal reaction of dirhodium tetraacetate and the phosphine $P(BrC_6H_4\text{-}1,2)(C_6H_5)_2$ in acetic acid. The structure of this compound has been determined by X-ray diffraction; it crystallizes in the $P\bar{1}$ (triclinic) space group and contains three acetate groups bridging a Rh_2^{4+} unit the Rh–Rh distance being 2.432(1)Å; the fourth bridging ligand is an *ortho*-bromophenyldiphenylphosphine metallated at one of the *ortho* positions of the unsubstituted phenyl rings. Two molecules of acetic acid occupy the axial coordination positions. Stepwise exchange of $CH_3CO_2^-$ by $CD_3CO_2^-$ is observed in $CDCl_3/CD_3CO_2D$ mixtures. The first step involves a fast exchange of the acetate group *trans* to the metallated phosphine and exchange of the two axial molecules of acetic acid. In a second step, the two acetate groups *cis* to the metallated phosphine slowly exchange with CD_3CO_2D at two different rates. The kinetics of the two slow processes have been studied by ^1H NMR spectroscopy using different $CDCl_3/CD_3CO_2D$ mixtures as solvent. The kinetic data follow rate laws of the type, $v = k[CD_3CO_2D]^{1/2}[Rh_2]$. At 298 K, the rate constants are k_{2a} $(1.86 \pm 0.02) \times 10^{-6}$ s^{-1} $M^{-1/2}$ ($\Delta H^{\ddagger} = 103 \pm 3$ kJ mol^{-1}; $\Delta S^{\ddagger} = -7 \pm 9$ J K^{-1} mol^{-1}) and $k_{2b} = (0.77 \pm 0.01) \times 10^{-6}$ s^{-1} $M^{-1/2}$ ($\Delta H^{\ddagger} = 100 \pm 6$ kJ mol^{-1}; $\Delta S^{\ddagger} = -20 \pm 20$ J K^{-1} mol^{-1}). Electrophilic attack at one oxygen atom of the bridging acetate by a protonated acetic acid species is assumed to be the first and rate-determining step. The unimolecular rate constant observed for the analogous compound with triphenylphosphine is negligible in this case, probably due to the low lability of the single axial acetic acid.

1. Introduction

It has been reported [1–5] that dirhodium tetraacetate reacts thermally with arylphosphines to give compounds where one or two acetates have been replaced by arylphosphine anions (PC^-) forming singly and doubly metallated compounds. Such reactions are usually performed in the presence of acetic acid or even in pure acetic acid [1]. Under such conditions labilisation and exchange of the bridging acetates with the reaction medium have to be considered even if such processes do not have any influence on the reaction stoichiometry unless a different carboxylic acid is used. A confirmation of this is the reaction of $[Rh_2(O_2CCH_3)_4]$ with $PMe_2(C_6H_5)$ in pivalic acid that yields $[Rh_2(O_2CCMe_3)_2\{(C_6H_4)PMe_2\}_2(HO_2CCMe_3)_2]$ [6].

The exchange of acetate for trifluoroacetate groups in $Rh_2(O_2CCH_3)_4$ was reported some years ago [7]. We have recently investigated the exchange of acetate groups with CD_3CO_2D in the monometallated compound $[Rh_2(O_2CCH_3)_3\{(C_6H_4)P(C_6H_5)_2\}(HO_2CCH_3)_2]$ [8]. The acetate group *trans* to the metallated phosphine and the two axial molecules of acetic acid exchange very fast, while the two acetate groups *cis* to the metallated phosphine exchange with CD_3CO_2D much more slowly. The kinetics of this slow process

Correspondence to: Professor P. Lahuerta or Dr. S. García-Granda.

0022-328X/93/$6.00

gave a rate law of the type $v = \{k_1 + k_2[CD_3CO_2D]^{1/2}\}[Rh_2]$.

We report in this paper the preparation and crystal structure determination of the compound $[Rh_2(O_2CCH_3)_3\{(C_6H_4)P(BrC_6H_4\text{-}1,2)(C_6H_5)\}(HO_2CCH_3)_2]$ (**2**). The kinetic study of the exchange of acetate groups with CD_3CO_2D in $[Rh_2(O_2CCH_3)_3\{(C_6H_4)P(BrC_6H_4\text{-}1,2)(C_6H_5)\}(HO_2CCH_3)]$ (**1**) shows that this exchange reaction takes place *via* a bimolecular process only.

2. Experimental details

2.1. Procedures and materials

$[Rh_2(O_2CCH_3)_4(MeOH)_2]$ was prepared according to literature methods [9]. Commercially available $P(BrC_6H_4\text{-}1,2)(C_6H_5)_2$ (Aldrich), $CDCl_3$ and CD_3CO_2D (acetic acid-d_4) were used as purchased. ^1H NMR measurements were recorded on a Bruker AC-200 spectrometer. All solvents were of analytical grade. Chloroform and toluene were dried and degassed before use: acetic acid was degassed.

2.2. Synthesis of 1 and 2

$[Rh_2(O_2CCH_3)_4(MeOH)_2]$ (100 mg, 0.198 mmol) and of $P(BrC_6H_4\text{-}1,2)(C_6H_5)_2$ (87 mg, 0.198 mmol) were dissolved in 50 ml of acetic acid. The resulting brown solution was heated under reflux for 45 min and it turned to deep blue. The solvent was removed under vacuum and the crude solid was dissolved in 5 ml of CH_2Cl_2hexane (1:1). The solution was column chromatographed (1.5×30 cm^2, silica gel/hexane). Elution with CH_2Cl_2/hexane (1:1) gave a minor yellow band which was discarded. Further elution with CH_2Cl_2/hexane/CH_3CO_2H (10:1:2) gave a deep blue band which was collected. The solvent was removed under reduced pressure and the solid **1** was crystallized from a mixture of CH_2Cl_2/hexane (yield 75%). To obtain good analytical data, this crystallization had to be repeated several times. ^1H NMR ($CDCl_3$) spectrum: 1.15 (3H, CH_3, s); 1.48 (3H, CH_3, s); 2.17 (3H, CH_3, s); 2.24 (3H, CH_3, s); 6.7–7 (13H, aromatics, m) ppm. $^{31}P\{^1H\}$ NMR (CH_2Cl_2) spectrum: $\delta p_a = 24.9$ ppm, ^1J(Rh–Pa) = 145.5 Hz, ^2J(Rh–Pa) = 6 Hz. Anal. Found: C, 39.73; H, 3.08. $Rh_2PBrC_{26}H_{26}O_8$ calcd.: C, 39.82; H, 2.98%.

Crystals of the bisadduct **2** suitable for X-ray studies were obtained by slow diffusion of hexane into a solution of **1** in a 1:1 CH_2Cl_2/HO_2CCH_3 mixture.

2.3. Kinetic measurements

Kinetics of exchange of 1 with acetic acid-d_4 40 mg (0.05 mmol) of **1** were added to an NMR tube. The solid was dissolved in 0.7 ml of a mixture of $CDCl_3/CD_3CO_2D$ of different compositions. The probe of the NMR spectrometer was equilibrated successively at 298, 308 and 318 K. The reaction progress was monitored by recording ^1H NMR spectra of the sample every 5–30 min depending on the reaction rates, by the decrease of the signals at 1.15 and 1.48 ppm corresponding to the *cis* $CH_3CO_2^-$ groups. The total intensity of all the methyl resonances, $\Sigma i(CH_3)$, was taken as the internal reference. This value corresponds to 4 methyl groups per mol of rhodium dimer. The percentage of protonated *cis* methyl groups is given by $100R$, with $R = 4[i(CH_3CO_2^- cis)/\Sigma i(CH_3)]$. The plot of InR *vs.* time was linear with correlation coefficients within the range 0.992–0.999. Activation parameters were calculated from the corresponding Eyring plots of the data obtained at different temperatures.

2.4. Crystal data

$C_{28}H_{30}BrO_{10}PRh_2$, $M_r = 843.23$, triclinic, space group $P\bar{1}$, $a = 11.228(1)$Å, $b = 11.714(4)$Å, $c = 14.472(1)$Å, $\alpha = 79.76(1)°$, $\beta = 68.00(1)°$, $\gamma = 64.70(1)°$, $V = 1595.3(6)$ Å^3, $Z = 2$, $D_x = 1.76$ g cm^{-3}. Mo Kα radiation (graphite crystal monochromator, $\lambda = 0.71073$ Å), μ(Mo Kα) = 23.59 cm^{-1}, $F(000) = 836$, $T = 293$ K.

2.5. X-Ray crystallographic procedures

A well-formed blue crystal of the compound grown by slow diffusion of hexane into a solution of **1** in a 1:1 CH_2Cl_2/HO_2CCH_3 mixture was used for the structure determination. X-Ray diffraction data were collected on an Enraf-Nonius CAD4 single-crystal diffractometer using graphite-monochromated Mo Kα radiation. Unit cell parameters were determined from the angular settings of 25 reflections with $15° < \theta < 20°$. A triclinic cell was obtained and the space group $P\bar{1}$ was confirmed from structure determination. A total of 5808 reflections were measured, *hkl* range (−13, −13, 0) to (13, 13, 31) and θ limits $0° < \theta < 25°$, using the ω–2θ scan technique and a variable scan rate with a maximum scan time of 60 s per reflection. Intensity was checked throughout data collection by monitoring three standard reflections every 60 min. Final drift corrections were between 0.97 and 1.02. Profile analysis was performed on all reflections [10,11]. Empirical absorption correction was applied using Ψ-scans [12], correction factors ranged from 0.93 to 1.00. Some Friedel pairs were averaged, $R_{int} = \Sigma(|I| - <I>)/\Sigma I = 0.012$, resulting in 5564 unique reflections, 4626 of which were 'observed' with $I > 3\sigma(I)$. Lorentz and polarization corrections were applied and data reduced to $|F_o|$-values.

The structure was solved by Patterson Interpretation using the SHELX86 program [13] and completed by DIRDIF [14]. Isotropic least-squares refinement using

SHELX76 [15] was performed until convergence. An additional empirical absorption correction was applied [16], with maximum and minimum correction factors of 1.50 and 0.75. Further anisotropic refinements followed by a difference Fourier synthesis allowed the location of most of the hydrogen atoms. Positional parameters and anisotropic thermal parameters of the non-hydrogen atoms were refined. All hydrogen atoms were refined isotropically riding on their parent atoms with a common thermal parameter.

Final conventional agreement factors were $R = 0.036$ and $R_w = 0.041$ for the 4626 'observed' reflections and 384 variables. The function minimized was $\Sigma w (F_o\text{-}F_c)^2$, $w = 1/[\sigma^2(F_o) + 0.00010F_o^2]$. The final difference Fourier map showed no peaks higher than 0.74 e Å^{-3} nor deeper than -1.23 e Å^{-3}. Atomic scattering factors were taken from International Tables for X-Ray Crystallography [17]. Geometrical calculations were performed with PARST [18]. Drawings were made using the EUCLID package [19]. All calculations were made on a MicroVax-3400 at the Scientific Computer Center, University of Oviedo and on a VAX 4000 at the Departamento de Química Física of the University of Valencia

Lists of structure amplitudes, anisotropic thermal parameters, H-atom parameters, distances and angles involving H atoms, distances, angles and least-square planes data and principal torsion angles are deposited with the Cambridge Crystallographic Data Centre.

3. Results

The thermal reaction of dirhodium tetraacetate with the phosphine $P(BrC_6H_4\text{-}1,2)(C_6H_5)_2$ in acetic acid gives the monometallated compound $[Rh_2(O_2CCH_3)_3\{(C_6H_4)P(BrC_6H_4\text{-}1,2)(C_6H_5)\}(HO_2CCH_3)]$ (**1**). In the presence of large concentrations of acetic acid (*ca.* 50% in volume) it forms a bisadduct of acetic acid,

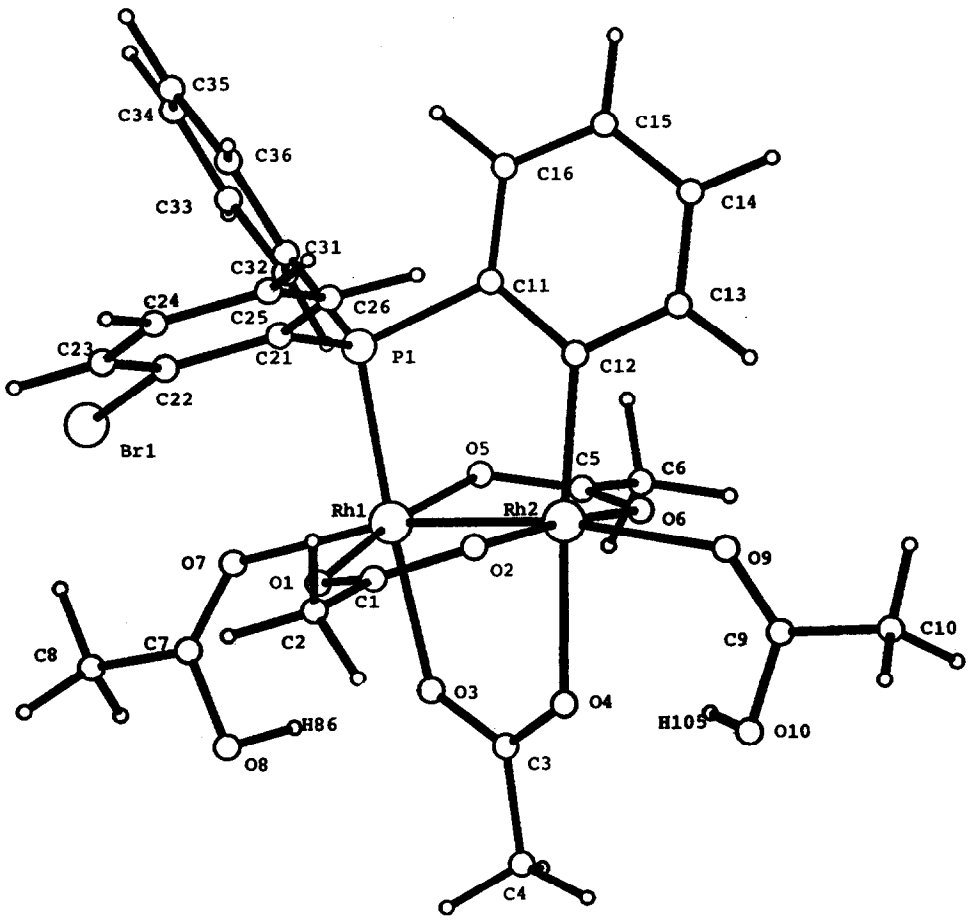

Fig. 1. Perspective view and atomic numbering scheme of compound **2**.

$[Rh_2(O_2CCH_3)_3[(C_6H_4)P(BrC_6H_4\text{-}1,2)(C_6H_5)](HO_2CCH_3)_2]$ (2), with one $(C_6H_4)P(o\text{-}BrC_6H_4)(C_6H_5)^-$ and three acetate groups bridging the Rh_2^{4+} unit.

3.1. Molecular structure of 2

A view of the structure is shown in Fig. 1. Important bond distances and angles are listed in Table 1, and atomic coordinates in Table 2. The two Rh atoms are bridged by three acetate groups and by one phosphine metallated in one of the two phenyl rings; two oxygens of two acetic acid molecules occupying the two axial positions complete the distorted octahedral coordination (angles in the range of 80.3(1)–104.0(1)) around the rhodium atoms.

The value of the Rh–Rh bond distance, 2.432(1) Å, is similar to those reported for monometallated compounds [2,3,20]. As judged by the torsion angles about the rhodium–rhodium bond (12.2(2)–18.9(2)°), the rhodium atoms are far from a totally eclipsed configuration. The Rh–Rh–O axial angles 166.0(1)° and 171.2(1)°, deviate from linearity, as in other monometallated complexes [2,3,20]. The Rh(1)–P and Rh(2)–C(12) bond distances are comparable to those found in other monometallated compounds [20]. The Rh–O bond *trans* to carbon, 2.220(3) Å, is longer than that *trans* to the P atom, 2.152(3) Å, consistent with the expected order of *trans* influences of M–C and M–P bonds. These bonds are much longer than the other four involving bridging-acetate ligands [2.030(4)–2.053(3) Å]. One of the axial Rh–O bonds (Rh(1)–O(7)) is considerably longer (2.434(4) Å) than the other (Rh(20–O(9) = 2.274(4) Å) and even longer than other reported distances of this type. This lengthening is indicative of some steric hindrance produced by the bromine atom of the phosphine, which is not in the coordination sphere of the rhodium.

The OH group of the axial acetic acid molecule with the shortest Rh–O distance interacts with the oxygen atom of the two bridging acetate *trans* to the metallated phosphine, forming an intramolecular hydrogen bond (H(105) $\cdots$ O(4) = 1.727(5) Å), while no H-bond was observed in the case of the axial molecule with the longest Rh–O distance.

The product resulting from crystallization from a CH_2Cl_2/hexane solution of **1** has an ^1H NMR spectrum consistent with the presence of only one acetic acid per rhodium dimer. This spectrum shows four signals in the methyl region at 2.24 (3H, $CH_3CO_2^-$ *trans* to PC^-), 2.17 (3H, axial CH_3CO_2H), 1.48 ppm (3H, $CH_3CO_2^-$ *cis* to PC^-) and 1.15 ppm (3H, $CH_3CO_2^-$ *cis* to PC^-). This assignment is based on previous NMR studies made for other monometallated compounds [2,3,20]. The observation of different chemical shifts for the two *cis* acetate bridges is due to the lack of symmetry in the metallated phosphine.

3.2. Exchange reactions

When **1** is dissolved in a mixture of $CDCl_3/CD_3CO_2D$, the ^1H NMR signal due to the *trans* $CH_3CO_2^-$ group disappears immediately, while the two signals due to the *cis* acetate groups remain unchanged. The ^1H NMR spectrum of a freshly prepared sample shows signals at 1.48 and 1.15 ppm due to the *cis* acetate groups and at 2.14 ppm due to the *trans* acetate group and the axial acetic acid rapidly exchanging with free acetic acid. After 5 min stirring, the sample was precipitated with hexane. The ^1H NMR ($CDCl_3$ solution) of the isolated solid shows that complete exchange of the

TABLE 1. Selected bond lengths (Å) and angles (°) with e.s.d.s for **2**

Rh1–Rh2	2.432(1)	Rh1–P1	2.216(1)	Rh1–O1	2.044(3)
Rh1–O3	2.152(3)	Rh1–O5	2.054(3)	Rh1–O7	2.434(4)
Rh2–O2	2.044(3)	Rh2–O4	2.220(3)	Rh2–O6	2.030(4)
Rh2–O9	2.273(4)	Rh2–C12	1.982(4)	Br1–C22	1.887(5)
P1–Rh1–Rh2	89.50(1)		O1–Rh1–Rh2		87.4(1)
O1–Rh1–P1	90.8(1)		O3–Rh1–Rh2		86.3(1)
O3–Rh1–P1	175.7(1)		O3–Rh1–O1		87.9(1)
O5–Rh1–Rh2	87.0(1)		O5–Rh1–P1		93.9(1)
O5–Rh1–O1	172.7(1)		O5–Rh1–O3		87.0(1)
O7–Rh1–Rh2	166.0(1)		O7–Rh1–P1		104.0(1)
O7–Rh1–O1	96.0(1)		O7–Rh1–O3		80.3(1)
O7–Rh1–O5	88.3(1)		O2–Rh2–Rh1		86.7(1)
O4–Rh2–Rh1	86.1(1)		O4–Rh2–O2		87.1(1)
O6–Rh2–Rh1	87.1(1)		O6–Rh2–O2		172.1(1)
O6–Rh2–O4	87.6(1)		O9–Rh2–Rh1		171.3(1)
O9–Rh2–O2	91.7(1)		O9–Rh2–O4		85.3(1)
O9–Rh2–O6	93.6(1)		C12–Rh2–Rh1		95.8(1)
C12–Rh2–O2	97.9(2)		C12–Rh2–O4		174.8(2)
C12–Rh2–O6	87.7(2)		C12–Rh2–O9		92.9(2)

TABLE 2. Fractional positional and thermal parameters (with e.s.d.s)

Atom	x	y	z	U_{eq}
Rh1	0.06439(3)	0.25945(3)	0.84145(3)	3.60(2)
Rh2	0.25873(4)	0.26300(4)	0.69292(3)	3.96(2)
Br1	−0.33605(6)	0.40701(6)	0.91055(4)	6.57(3)
P1	−0.0348(1)	0.2285(1)	0.74686(9)	3.47(5)
O1	−0.0287(3)	0.4507(3)	0.8228(2)	4.6(1)
O2	0.1313(4)	0.4441(3)	0.6693(3)	5.0(2)
O3	0.1711(3)	0.2935(4)	0.9232(2)	5.3(2)
O4	0.3175(4)	0.3431(4)	0.7890(3)	5.4(2)
O5	0.1814(3)	0.0705(3)	0.8551(3)	5.1(2)
O6	0.3736(3)	0.0891(4)	0.7366(3)	5.4(2)
O7	−0.0906(4)	0.2492(4)	1.0107(3)	6.1(2)
O8	−0.0467(6)	0.3676(6)	1.0876(4)	11.8(4)
O9	0.4464(4)	0.2827(4)	0.5683(3)	6.5(2)
O10	0.5315(4)	0.3611(5)	0.6456(3)	8.2(3)
C1	0.0218(5)	0.5002(5)	0.7405(4)	4.9(2)
C2	−0.0581(6)	0.6389(5)	0.7229(5)	6.7(3)
C3	0.2703(6)	0.3291(5)	0.8820(4)	5.4(3)
C4	0.3314(7)	0.3572(8)	0.9466(5)	9.1(4)
C5	0.3111(5)	0.0308(5)	0.8071(5)	5.5(3)
C6	0.3993(7)	−0.0981(6)	0.8393(6)	8.6(4)
C7	−0.1141(6)	0.3014(7)	1.0838(5)	6.8(3)
C8	−0.2086(8)	0.2874(9)	1.1852(5)	11.1(5)
C9	0.5332(5)	0.3201(6)	0.5672(4)	5.8(3)
C10	0.6535(7)	0.3198(7)	0.4747(5)	8.1(2)
C11	0.0985(5)	0.1580(5)	0.6321(4)	4.4(2)
C12	0.2219(5)	0.1774(4)	0.6065(3)	4.1(2)
C13	0.3278(5)	0.1238(5)	0.5165(4)	5.3(2)
C14	0.3078(6)	0.0585(6)	0.4575(4)	6.5(3)
C15	0.1860(6)	0.0439(6)	0.4821(4)	7.0(3)
C16	0.0810(6)	0.0906(6)	0.5705(4)	6.5(3)
C21	−0.1558(4)	0.3726(4)	0.7071(3)	3.9(2)
C22	−0.2820(5)	0.4499(5)	0.7735(4)	4.8(2)
C23	−0.3741(6)	0.5603(6)	0.7452(6)	7.2(3)
C24	−0.3411(7)	0.5991(7)	0.6461(7)	8.6(4)
C25	−0.2164(8)	0.5254(7)	0.5770(5)	7.7(4)
C26	−0.1239(6)	0.4148(5)	0.6069(4)	5.4(2)
C31	−0.1365(5)	0.1305(4)	0.7961(3)	4.0(2)
C32	−0.1114(5)	0.0423(5)	0.8721(4)	5.3(3)
C33	−0.1884(6)	−0.0340(6)	0.9086(5)	6.9(3)
C34	−0.2880(6)	−0.0196(6)	0.8699(5)	6.9(3)
C35	−0.3164(5)	0.0687(5)	0.7954(4)	5.6(3)
C36	−0.2393(5)	0.1436(5)	0.7584(4)	4.8(2)

trans acetate and the axial acetic acid by the deuterated groups has occurred.

Slow exchange of the *cis* acetate groups is observed with **1** in solution in a $CDCl_3/CD_3CO_2D$ mixture at room temperature for several hours, as already described for a related monometallated compound [8]. The kinetics of this slow process show two different rates for the exchange of the two different *cis* acetate groups.

3.3. Kinetic study

The slow carboxylate exchange process has been studied kinetically by ^1H NMR spectroscopy, monitoring the disappearance of the signals at 1.48 and 1.15 ppm corresponding to the *cis* acetate groups, in chloroform solutions of constant concentration of **1** with concentrations of CD_3CO_2D.

TABLE 3. Observed values of k_a and k_b at different temperatures and concentrations of CD_3CO_2D

$[CD_3CO_2D](M)$	0.00	0.51	2.34	4.68	9.35	14.08
$T = 298$ K						
10^5k_a (s^{-1})	0.00	–	–	0.37	0.55	0.70
10^5k_b (s^{-1})	0.00	–	–	0.12	0.22	0.55
$T = 308$ K						
10^5k_a (s^{-1})	0.00	–	–	1.68	2.51	2.99
10^5k_b (s^{-1})	0.00	–	–	0.88	1.39	1.68
$T = 318$ K						
10^5k_a (s^{-1})	0.00	2.26	4.59	6.93	9.15	11.60
10^5k_b (s^{-1})	0.00	1.26	2.61	3.73	5.63	7.56

$$[Rh_2(O_2CCH_3)_{2cis}(O_2CCD_3)_{trans}\{PC\}(DO_2CCD_3)] + 2DO_2CCD_3 \longrightarrow [Rh_2(O_2CCD_3)_{2cis} \times (O_2CCD_3)_{trans}\{PC\}(DO_2CCD_3)] + 2HO_2CCH_3$$

This has already been described for the monometallated compound $[Rh_2(O_2CCH_3)_3\{(C_6H_4)P(C_6H_5)_2\}(HO_2CCH_3)_2]$ in a recent publication [8].

By the procedure described in the experimental section, we obtained k_{obs} values from the slopes of the plots of $\ln R_a$ and $\ln R_b$ *vs.* time, in which $R_a = 1/4[i(CH_3CO_2^-cis_a)/[\Sigma i(CH_3)]$ and $R_b = 1/4[i(CH_3CO_2^-cis_b)/[\Sigma i(CH_3)]$ (a and b being the two different *cis* acetate bridges). As changes in the concentration of **1** do not lead to any significant change in the observed rate constants k_a and k_b, we assume that the reaction is first-order in **1**. The reaction was performed at different concentrations of acetic acid-d_4 and different

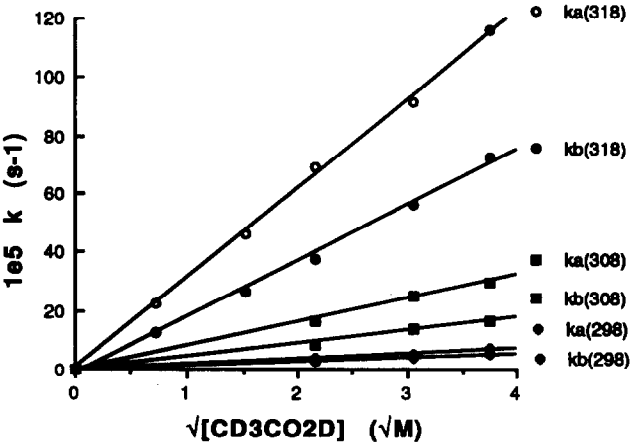

Fig. 2. Plots of k_{2a} and k_{2b} *vs.* $[CD_3CO_2D]^{1/2}$ for the exchange of acetate groups between **1** and $CD_3CO_2^-$.

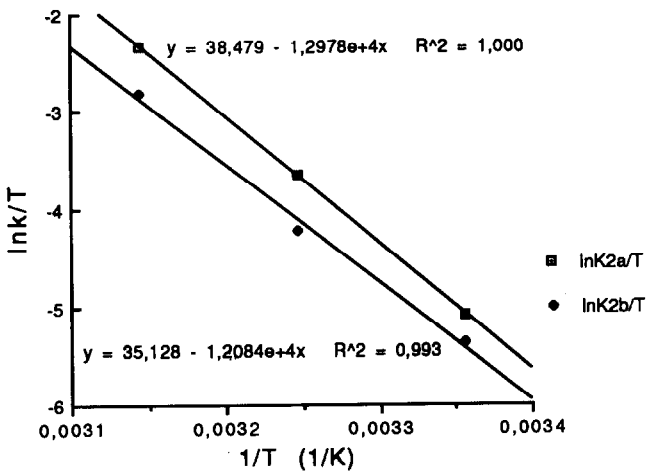

Fig. 3. Standard Eyring plots for the intermolecular mechanism of exchange of acetate groups between **1** and $CD_3CO_2^-$.

temperatures. The observed rate constants obtained for the substitution of each acetate group are summarized in Table 3.

The plots of k_a and k_b against acetic acid-d_4 concentration (Fig. 2) were fitted to eqns. (1) and (2) with correlation coefficients of more than 0.99.

$$k_a = k_{2a}[CD_3CO_2D]^{1/2} \quad (1)$$

$$k_b = k_{2b}[CD_3CO_2D]^{1/2} \quad (2)$$

The second-order rate constants k_{2a} and k_{2b} are associated with intermolecular processes. We did not observe scrambling of the carboxylate groups between *cis* and *trans* positions when the partially deuterated compound $[Rh_2(O_2CCH_3)_{2cis}(O_2CCD_3)_{trans}\{(C_6H_4)P(BrC_6H_4\text{-}1,2)(C_6H_5)\}(DO_2CCD_3)]$ is dissolved in $CDCl_3$ in the absence of acetic acid-d_4.

From the values at different temperatures of k_{2a} and k_{2b}, we obtained standard Eyring plots (Fig. 3) from which we have calculated the activation parameters (Table 4).

TABLE 4. Values at different temperatures of k_{2a} and k_{2b}: activation parameters

T (K)	$10^6 k_{2a}$ (s^{-1} $M^{-1/2}$)	$\Delta H^{\neq}$ (kJ mol^{-1})	$\Delta S^{\neq}$ (kJ mol^{-1} K^{-1})
298	1.86		
308	8.05		
318	30.6	103±3	−7± 9
298	0.77		
308	4.49		
318	19.13	100±6	−20±20

4. Discussion

The above kinetic results show that **1** undergoes very rapid exchange of the *trans* acetate group and of the axial molecule of acetic acid with the acetic acid present in solution. The two *cis* acetate groups, which are magnetically non-equivalent, undergo slow exchange with acetic acid at different rates. This can be due to difference in the steric hindrance produced by the bromine atom of the metallated phosphine which is closer to one of the *cis* acetate groups. We assume that the *cis* acetate group which is closer to the bromine atom, labelled b in Scheme 1, will exchange more slowly than the other (a).

These results must be compared with those obtained for the exchange reaction of the monometallated compound with triphenylphosphine [8]. In both systems, the reaction rate depends on the square root of the total acetic acid concentration due to the weak dissociation of CD_3CO_2D in chloroform-*d* solution according to $2CD_3CO_2D \leftrightarrow CD_3CO_2D_2^+ + CD_3CO_2^-$. The main difference in the kinetics of these two systems is that the rate law for **2** does not contain the unimolecular term observed for the triphenylphosphine compound. If we take into account that a factor of 2 has to be applied to the observed constant rates in **1**, due to a probability factor (we measure the substitution of individual *cis* acetate bridges), k_{2a} ($1.86 \pm 0.03 \times 10^{-6}$ s^{-1} $M^{-1/2}$) is identical to the intermolecular rate constant k_2 in the triphenylphosphine analogue compound ($3.83 \pm 0.01 \times 10^{-6}$ s^{-1} $M^{-1/2}$; for the substitution of two equivalent *cis* acetate bridges). However, k_{2b} is reduced by a factor of 2.5, due to the probable steric influence of the bromine atom. The activation parameters $\Delta H^{\neq}$ and $\Delta S^{\neq}$ are similar for both compounds. Analogous monometallated compounds containing Cl and $(C_5H_4)Fe(C_5H_5)$ groups instead of Br also show different rates of substitution of the two *cis* acetate groups [21].

The suggested reaction mechanism presented in Scheme 1 is similar to that described for the triphenylphosphine compound, without the intramolecular path. The intermolecular process is described as (i) concerted transfer of one D^+ from one protonated acetic acid to one oxygen of the bridging group followed by (ii) cleavage of the Rh–O bond of the protonated acetate with coordination of one acetate group. As we saw in the triphenylphosphine compound, the substitution of the *trans* acetate group is as fast as that of the axial ligands, maybe due to the *trans* influence induced by the metallated phosphine.

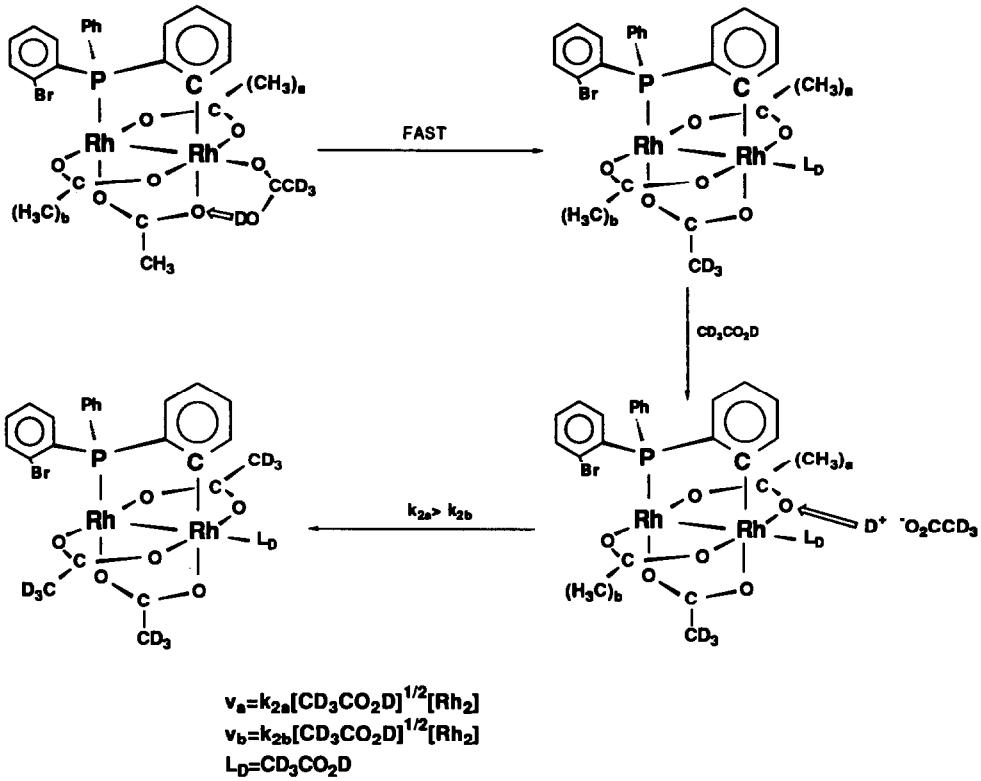

Scheme 1.

Two possible interpretations were given for the intramolecular process observed in our previous studies. The first was to assume that the axial carboxylic acid can rotate around the Rh–O bond, interacting with the *cis* acetate group. The alternative was to assume that the axial acetic acid undergoes Rh–O bond cleavage prior to the attack. The results presented in this paper support the idea that the unimolecular process must be the result of the breaking of the axial Rh–O bond.

The crystal structure shows that compound **2** contains one axial molecule of acetic acid more strongly bonded than the other, which is closer to the bromine atom of the metallated phosphine. Crystals of compound **2** with both axial acetic acid molecules are only obtained if a large concentration (*ca.* 50% in volume) of acetic acid is present in solution.

As a result, the less sterically hindered axial molecule of acetic acid must be more strongly bonded, and consequently less labile than in other bis(adduct) species such as $[Rh_2(O_2CCH_3)_3\{(C_6H_4)P(C_6H_5)_2\}(HO_2CCH_3)_2]$. The lack of a unimolecular term in the rate law for the exchange of carboxylate ligands in **1** is attributed to the relatively lower lability of the unique axial acetic acid in this monoadduct.

Acknowledgements

We are grateful to the C.I.C.Y.T. for financial support and to Dr. Manel Martínez for his interest and comments in this work.

References

1 A.R. Chakravarty, F.A. Cotton D.A. Tocher and J.H. Tocher, *Organometallics, 4,* (1985) 8.
2 P. Lahuerta, J. Payá, X. Solans and M.A. Ubeda *Inorg. Chem., 31* (1992) 385.
3 P. Lahuerta, J. Payá, M.A. Pellinghelli and A. Tiripicchio, *Inorg. Chem., 31* (1992) 1224.
4 (a) E.C. Morrison and D.A. Tocher, *J. Organomet. Chem., 408* (1991) 105; (b) P. Lahuerta, R. Martínez-Máñez, J. Payá, E. Peris and W. Díaz, *Inorg. Chim. Acta, 173* (1990) 99.
5 P. Lahuerta, J. Payá, E. Peris, A. Aguirre, S. García-Granda and F. Gómez-Beltrán, *Inorg. Chim. Acta, 192* (1992) 43.
6 E.C. Morrison and D.A. Tocher, *Inorg. Chim. Acta, 157* (1989) 139.
7 J.L. Bear, J. Kitchens and M.R. Wilcott, *J. Inorg. Nucl. Chem., 33* (1971) 3479.
8 P. Lahuerta, and E. Peris, *Inorg. Chem., 31* (1992) 4547.
9 G.A. Rempel, P. Legzdins, H. Smith and G. Wilkinson, *Inorg. Synth., 13* (1972) 9.

10 M.S. Lehman and F.A. Larsen, *Acta Crystallogr., Sect. A, 30* (1974) 580.
11 D.F. Grant and E.J. Gabe *J. Appl. Crystallgr., 11* (1978) 114.
12 A.C.T. North, J.C. Phillips and F.S. Mathews *Acta Crystallogr., Sect. A, 24* (1968) 351.
13 G.M. Sheldrick, C. Kruger and R. Goddard (eds.) *Crystallographic Computing*, Clarendon Press, Oxford, 1985, p. 175.
14 P.T. Beurskens, G. Admiraal, G. Beurskens, W.P. Bosman, S. García-Granda, R.O. Gould, J.M.M. Smits and C. Smykalla, The DIRDIF program system, *Technical Report of the Crystallography Laboratory*, University of Nijmegen, The Netherlands, 1992.
15 G.M. Sheldrick, SHELX76, Program for Crystal Structure Determination, University of Cambridge, 1976.
16 N. Walker and D. Stuart, *Acta Crystallogr., Sect. A, 39* (1983) 158.
17 *International Tables for X-Ray Crystallography*, Vol. IV, Kynoch Press, Birmingham, 1974. (present distributor Kluwer, Dordrecht).
18 M. Nardelli, *Comput. Chem., 7* (1983) 95.
19 A.L. Spek, The EUCLID package, in D. Sayre (ed.), *Computational Crystallography*, Clarendon Press, Oxford, 1952, p. 528.
20 (a) P. Lahuerta, J. Payá, E. Peris, M.A. Pellinghelli and A. Tiripicchio, *J. Organomet. Chem., 373* (1989) C5; (b) P. Lahuerta, J. Payá, S. García-Granda, F. Gómez-Beltrán and A. Anillo, *J. Organomet. Chem., 443* (1993) C14; (c) P. Lahuerta, J. Latorre, E. Peris, M. Sanaú, M.A. Ubeda and S. García-Granda, *J. Organomet. Chem., 445* (1993) C10.
21 P. Lahuerta *et al.*, unpublished results.